Harmonic content of the synchronous generator stator current in the case of unit transformer saturation due to geomagnetically induced currents

Vera Vakhnina, *Aleksei* Kuvshinov, *Aleksei* Chernenko *, and *Roman* Pudovinnikov

Togliatti State University, 445020 Togliatti, Russia

Abstract. The study investigates the features of the operation of off-the-grid power systems. Such power systems are commonly used for supplying power to consumers spread throughout the Arctic zone of the Russian Federation, and their unique operating conditions are due to the effect of geomagnetically induced currents (GICs) resulting from geomagnetic disturbances. We argue that the cause of stator current deviations from the pure sine wave are unit transformers. Their low-voltage windings are directly connected to stator windings of synchronous generators, and GICs run through grounded high-voltage windings. To support our claim, we simulated the effect of a test GIC event. Its amplitude in each of high-voltage phase windings of the unit transformer was 100 A, and the duration was 20 seconds (power transformers of the Hydro-Québec power grid were exposed to geomagnetically induced currents of a similar intensity during the geomagnetic storm on March 13-14, 1989). The spike targeted the "generator (TVF-100-2) - transformer (TDTs-125000/220/10.5)" unit that fed a major consumer node (Pnom = 83.125 MW, Qnom = 29.75 Mvar, cosφ=0.95) through a 160 km long double-circuit overhead line. Our study demonstrated that the effect of GICs on the operation of synchronous generators started from the moment of saturation of the unit transformer's core due to the inverse transformation of magnetizing current harmonics in the stator winding circuit. The harmonics introduced significant deviations from the pure sine wave into the curve of instantaneous stator currents. We calculated the nonlinear distortion factor of the stator current, which reached an unacceptably high value of THD=55.59%, 10 seconds into the test GIC event. The study showed that the 2nd and 4th harmonics of the unit transformer magnetizing current were responsible for the great bulk of deviations from the pure sine wave of the stator current.

* Corresponding author: tchernenko83@yandex.ru

1 Introduction

Currently, the largest, most significant, and best-performing electric power project in Russia is the project of electrification of its Arctic coast and islands, aimed at reliable and uninterrupted supply of electricity to all entities developing the Arctic zone of the Russian Federation. The Arctic zone of the Russian Federation is characterized by the presence of numerous consumers spread throughout the area, who are supplied with power by off-the-grid power systems. Such systems are vulnerable to the effect of geomagnetically induced currents (GIC) resulting from increased geomagnetic activity. When GICs with frequency of (0.001 - 0.1) Hz run through the grounded high-voltage windings of unit transformers at power plants, operating conditions required for the flux reversal of electrical steel shift to the region of technical saturation [1,2]. This causes one-way saturation of the magnetic system and a multifold increase in the magnetization current [3,4]. The latter takes an almost unipolar form with a wide range of both odd (3, 5, 7, 9, ...) and even (2, 4, 6, 8, ...) higher harmonics [5,6,7]. Unit transformers with shell-type and shell-core designs of the core are most sensitive to GIC effects. The transformers of this type are commonly used as part of units of 100 MVA and more [8,9]. Under geomagnetic disturbances, such unit transformers will emit higher harmonics of magnetizing current both in the stator winding circuit and into the adjacent electrical network. The above confirms the relevance of the task of investigating the harmonic content of the stator current of synchronous generators resulting from the saturation of the magnetic system of the unit transformer due to GICs. In this paper, we solve the problem as applied to the case of modeling an off-the-grid power system in the MATLAB environment [10].

2 Model of an off-the-grid power system

Fig. 1 shows the equivalent circuit of a standard off-the-grid power system. The "generator-transformer" unit formed by the synchronous generator G1 (turbo-generator of the TVF-100-2 type) and unit transformer T1 (TDTs-125000/220/10.5) feeds a major consumer node L (P_{nom} = 83, 125 MW, Q_{nom} = 29.75 Mvar, cosφ=0.95) through a double-circuit overhead transmission line (phase conductor grade - AS-400, line length - 160 km) and the autotransformer T2 (ATDTsTN-125000/220/110/10.5). The ohmic resistances R3 (the standard value is 0.5 ohms) model the grounding devices of the unit transformer T1 and autotransformer T2. The effect of GICs is modeled by the geoelectric field source G2 acting between the grounding devices of the unit transformer T1 and autotransformer T2.

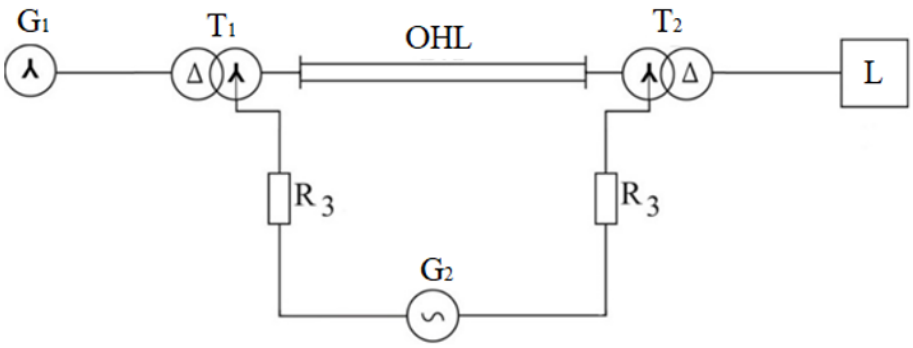

Fig. 1. Equivalent circuit of a standard off-the-grid power system.

Instrumental measurements indicated that the process of unfolding of real-life GICs over time is a sequence of unipolar spikes, which are characterized by random variation of both shape and parameters: the amplitude ranges from a few amperes to hundreds of amperes and duration ranges from tens of seconds to tens of minutes [11,12,13,14]. Under these conditions, a proper research tool is the use of a test GIC event acting as a disturbance, which reproduces only the main parameters of a real-life spike: its amplitude and duration. It makes sense to use an elementary function to capture instantaneous values of a test GIC spike. The nature of their change in this case is of secondary importance. The above requirements are reasonably satisfied by the representation of the geoelectric field source G2 by a harmonic function that creates a unipolar potential difference between the grounded neutrals of the unit transformer T1 and autotransformer T2.

$$e_{\mathrm{GIC}} = (E_{0(m)} \cdot l) \cdot |\sin(2\pi f_{\mathrm{GIC}} \cdot t)|, \quad (1)$$

where $E_{0(m)}$, f_{GIC} is the amplitude and frequency of change of the instantaneous values of the test spike of the geoelectric field strength of the G2 source, and l stands for the overhead line length.

3 Magnetizing current of the unit transformer

In the initial steady-state operation of the off-the-grid power system, the synchronous generator G1 serves an active load of P=83.78 MW with stator current of 4,607 A, and the power factor almost equal to unity. This is explained by the fact that the charging power of the double-circuit overhead line (46.08 Mvar) is sufficient to compensate for the reactive power of the consumption node L, reactive power loss in the unit transformer T1, autotransformer T2, as well as in the inductive reactances of the phase conductors of the overhead line. Under these conditions, the synchronous generator G1 is underexcited during its operation and even consumes a small amount of reactive power of about 0.833 Mvar. The magnetizing current (the effective value is 1.72 A) of the unit transformer T1 matches the nameplate data.

The moment of time t=0 s marks the start of the effect of a test spike of the geoelectric field strength of the form (1), the parameters of which are chosen to be ($E_{0(m)} = 6.94$ V/km, $f_{\mathrm{GIC}} = 0.05$ Hz) so that the amplitude of the GIC spike in each HV phase winding of the unit transformer is 100 A, and the duration of its flow is 20 seconds (similar in intensity to the GIC effects that power transformers of the Hydro-Québec power grid were subjected to during the geomagnetic storm on March 13-14, 1989 [15]).

Fig.2, a shows the nature of change of neutral current of the unit transformer T_1, which is determined only by the value of GICs up to the moment of time $t_{\mu(1)} = 4.3\ c$.

$$i_N = 3 \cdot I_{\mathrm{GIC}} \cdot \sin(2\pi f_{\mathrm{GIC}} \cdot t), \quad (2)$$

and then zero-sequence harmonics appear in the neutral current due to saturation of the core of the unit transformer T_1

$$i_N = 3 \cdot \left[I_{\mathrm{GIC}} \cdot \sin\left(2\pi f_{\mathrm{GIC}} \cdot t + \varphi_{\mu(1)}\right) + \sum_{n=1}^{\infty} I_{m(3n)}^{(t)} \cdot \sin\left(3n\omega \cdot t + \varphi_{(3n)}^{(t)}\right)\right], \quad (3)$$

where $\varphi_{\mu(1)} = 2\pi f_{\mathrm{GIC}} \cdot t_{\mu(1)}$ - phase angle of the test GIC, at which saturation of the magnetic system of the unit transformer T_1 begins (in this case $\varphi_{\mu(1)} \cong 38.7\ deg.$); $I_{m(3n)}^{(t)}$, $\varphi_{(3n)}^{(t)}$ - amplitude and initial phase of the *n*-th harmonic (3rd, 6th, 9th, etc.) of the zero-sequence magnetizing current at time *t* after the beginning of the test GIC effect.

Fig. 2,b shows the simulation result of the magnetizing current of the unit transformer T_1 at the exposure interval $(0-20)$s and the post-exposure interval $(20-25)$s of the test GIC spike. Several distinctive intervals are clearly visible, which is due to a feature of the standard Saturable Transformer component: the component take into account the saturation of the

magnetic system through a piecewise linear approximation of the relationship between the flux linkage and magnetizing current with two breakpoints.

The interval (0 - $t_{\mu(1)} = 4.3$ s) is characterized by the latent effect of GIC, where the magnetizing current of the unit transformer T_1 remains the same, but the flux linkage of HV windings becomes a sum of two components

$$\Psi_{\Sigma}(t) = \Psi_{\text{GIC}}(t) + \Psi_{U}(t). \quad (4)$$

$\Psi_{\text{GIC}}(t)$ - component of the flux linkage due to GIC in HV windings; $\Psi_{U}(t)$ - component of the flux linkage $\Psi_{U}(t)$, due to the voltage of HV windings.

In the design of power transformers, the amplitude value of the magnetic field induction in the core of the magnetic system is chosen to be equal to $B_m = (1.6 - 1.65)$T at the rated winding voltage, and the saturation induction value of most modern grades of high-quality electrical steel is $B_S \cong 2.0$T.

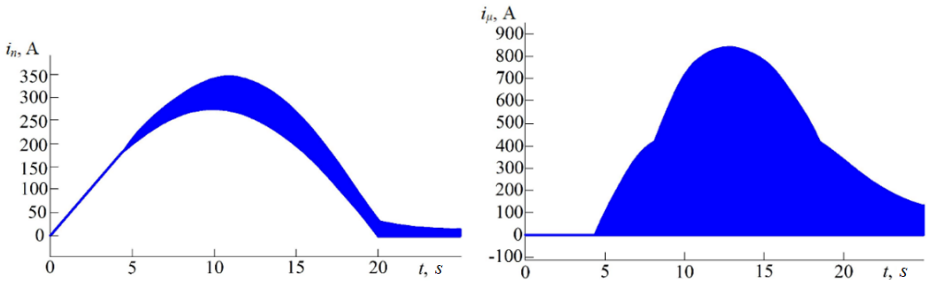

a) b)

Fig. 2. Neutral current (a) and magnetizing current (b) of the unit transformer at the exposure interval and after the end of the test GIC spike.

The real magnetization curve differs markedly from the linear relationship only in the inflection region and hence within a very narrow range of magnetic induction values $B = (0.95 - 1.03)B_S$ [8,9,16]. This feature is reproduced by the piecewise linear approximation with two breakpoints, which is adopted in the standard Saturable Transformer block. As the first breakpoint we can take $B_{S(1)} = 0{,}95B_S$, and as the second break point we can take $B_{S(2)} = 1.03B_S$. Hence the relations $B_{S(1)}/B_m = (1.15 - 1.19)$ and $B_{S(2)}/B_m = (1.25 - 1.29)$ can be easily transformed into similarly-formed relations $\Psi_{S(1)}/\Psi_m = (1.15 - 1.19)$ and $\Psi_{S(2)}/\Psi_m = (1.25 - 1.29)$ for flux linkages (here $\Psi_{S(1)}$, $\Psi_{S(2)}$ – flux linkages of the HV winding, which correspond to the first and second breakpoints of the piecewise linear approximation of the magnetization characteristic of the unit transformer T_1, Ψ_m - amplitude value of the flux linkage of the HV winding at rated voltage).

At the moment of time $t = t_{\mu(1)}$, due to the increase of the flux-linkage component $\Psi_{\text{GIC}}(t)$ resulting from GIC, there comes the equality $\Psi_{\Sigma}(t_{\mu(1)}) = \Psi_{S(1)}$, which means the beginning of the saturation process of the magnetic system of the unit transformer T_1. The magnitude of the GIC at the moment of time $t = t_{\mu(1)}$ is 62.52 A.

At the interval of exposure to the test GIC spike from $t_{\mu(1)} = 4.3s$ up to $t_{\mu(2)} = 8.1s$, the initial saturation process takes place. The total flux linkage of the HV winding of the unit transformer T_1 falls within the limits of $\Psi_{S(1)} < \Psi_{\Sigma}(t) < \Psi_{S(2)}$, and the magnetizing current takes the shape shown in Fig. 3,a.

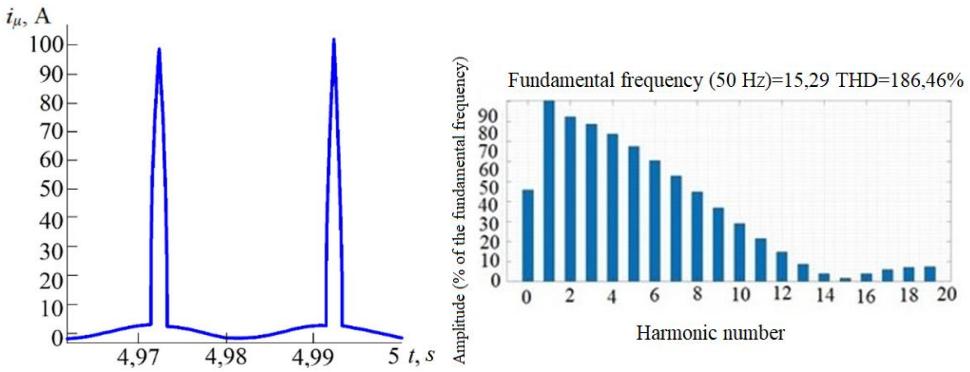

a) b)

Fig. 3. Time chart (a) and harmonic content (b) of magnetizing current in-rushes ≈5s into the GIC test exposure.

The instantaneous values $i_\mu(t)$ and amplitude $I_{\mu\,max}$ of the magnetizing current in-rushes shown in Fig. 3,a, can be determined by simple analytical expressions [17]:

$$i_\mu(t) = I_{m(\mu)} \cdot (cos\varphi + cos\omega t), \tag{5}$$

$$I_{\mu\,max} = I_{m(\mu)} \cdot (1 - cos\varphi) \tag{6}$$

where $I_{m(\mu)}$ - the magnetizing current amplitude in the case of saturation of the core of the unit transformer T_1 during the entire voltage cycle; $\varphi = \omega\tau_\varphi/2$ - the phase angle of saturation of the core of the unit transformer T_1.

Based on expressions (5), (6) it is possible to obtain analytical expressions for calculating the amplitudes of the n -th harmonic

$$I_{\mu\,(n)} = \left\{\frac{I_{\mu\,max}}{\pi\cdot(1-cos\varphi)} \cdot \left[\frac{\sin(n-1)\varphi}{(n-1)} + \frac{\sin(n+1)\varphi}{(n+1)} - \frac{2}{n} \cdot cos\varphi \cdot \sin(n\varphi)\right]\right\}, \tag{7}$$

and the fundamental frequency of the magnetizing current

$$I_{\mu\,(1)} = \frac{I_{\mu\,max}}{2\pi} \cdot \frac{(2\varphi - sin2\varphi)}{(1-cos\varphi)} \tag{8}$$

As can be seen in Fig. 3,b and as follows from expression (7), the harmonic content of the magnetizing current is represented by both odd (3rd, 5th, 7th, etc.) and even (2nd, 4th, 6th, etc.) harmonics. Moreover, the appearance of the latter serves as a telling indicator of one-way saturation of the core of the unit transformer T_1.

At the moment of time $t_{\mu(2)} = 8.1$s, the HV winding flux linkage reaches the value $\Psi_\Sigma(t) = \Psi_{S(2)}$ and the process of technical saturation of the core of the unit transformer T_1 begins, which continues until the moment of time $t_{\mu(3)} = 18.51$s. The interval $(_{\mu(2)} - t_{\mu(3)})$ is clearly visible in Fig. 2,b by the characteristic kink of the magnetizing current envelope. At this interval, the HV winding flux linkage is maintained by GICs in the technical saturation region when $\Psi_\Sigma(t) > \Psi_{S(2)}$. The time chart shown in Fig.4,a illustrates a characteristic kink in the shape of magnetizing current in-rushes during the transition from the region of initial saturation to the region of technical saturation.

By the time $t_{\mu(3)} = 18.51$ s the value of GIC decreases down to 23.2 A, causing the magnetizing current in-rush amplitude to decrease to 420 A, and the HV winding flux linkage to decrease down to $\Psi_\Sigma(t) = \Psi_{S(2)}$. The core of the unit transformer T_1 after the effect of the test GIC spike lasting for 20s will return to the initial state of normal operation with the nameplate magnetizing current after a time interval equal to ≈21,6s (Fig. 2,b does not show this interval).

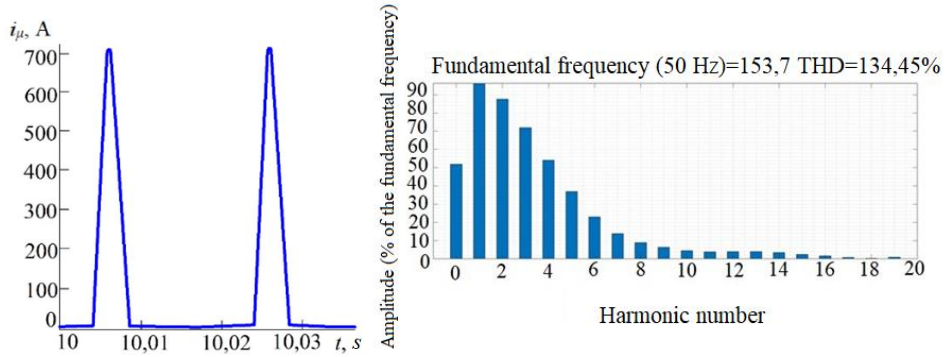

a) b)

Fig. 4. Time chart (a) and harmonic content (b) of magnetizing current in-rushes, ≈10s into the test GIC event.

4 Harmonic content of stator winding current of synchronous generators

A negative consequence of saturation of the core of the unit transformer T_1 is the emission of harmonics of the magnetizing current both to the low-voltage side in the stator winding circuit of the synchronous generator, and to the high-voltage side in the circuit of adjacent overhead lines. Fig.5 shows the time chart of instantaneous values (a) and harmonic content (b) of stator winding current of a synchronous generator.

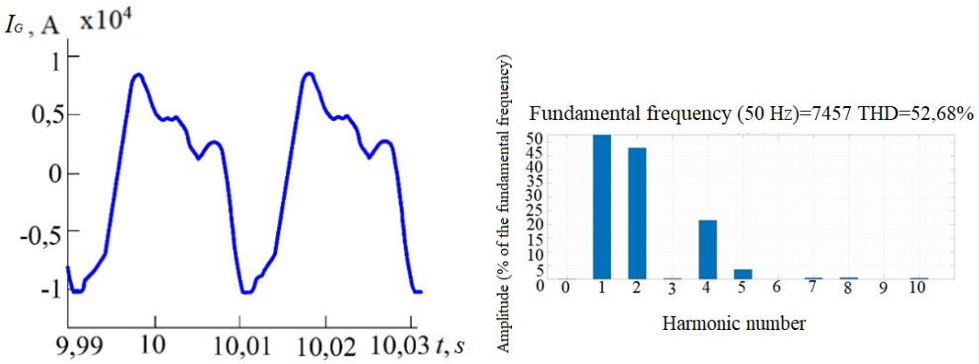

a) b)

Fig. 5. Graph of instantaneous values (a) and harmonic content (b) of stator current, 10s into test GIC event.

Comparison of the harmonic content of the magnetizing current of the unit transformer (Fig. 4, b) and the stator winding current of the synchronous generator (Fig. 5, b) for the same moment of time (10s into the test GIC event) confirms that the second and fourth harmonics appear only in the case of one-way saturation of the core of the unit transformer T_1.

The highest possible level of the effective value of the *n*-th harmonic of the stator current can be determined by the following relation in the case when the harmonics of the magnetizing current of the unit transformer T_1 are fully closed on the low-voltage side and run through the stator windings of the synchronous generator:

$$I_{\mathrm{G}(n)\mathrm{eff}}^{(\mathrm{lim})} = \sqrt{3} \cdot K_T \cdot I_{\mu(n)eff}, \quad (9)$$

where $I_{\mathrm{G}(n)\mathrm{eff}}^{(\mathrm{lim})}$ - the limit level of the effective value of the *n*-th harmonic of the stator current; $I_{\mu(n)\mathrm{eff}}$ - the effective value of the *n*-th harmonic of the magnetizing current of the unit transformer T_1; $K_T = U_{\mathrm{HV_L}}/U_{\mathrm{LV_L}}$ - the transformation ratio of the unit transformer T_1; $U_{\mathrm{HV_L}}, U_{\mathrm{LV_L}}$ - nominal voltages of the high- and low-voltage windings of the unit transformer T_1.

The limit level of the effective value of the *n*-th harmonic of the stator current $(I_{\mathrm{G}(n)\mathrm{eff}}^{(\mathrm{lim})})$, calculated as per expression (9), and the effective value of the *n*-th harmonic of the stator current $(I_{\mathrm{G}(n)\mathrm{eff}})$, determined by Fig. 5, b, allow us to determine the emission level of harmonics of the magnetizing current of the unit transformer T_1 into the circuit of adjacent overhead lines

$$I_{\mathrm{OHL}(n)\mathrm{eff}} = \frac{I_{\mathrm{G}(n)\mathrm{eff}}^{(\mathrm{lim})} - I_{\mathrm{G}(n)\mathrm{eff}}}{\sqrt{3}\cdot K_T}. \quad (10)$$

Table 1 presents numerical values of magnetizing current harmonics $I_{\mu(n)\mathrm{eff}})$, determined by Fig. 4, b; estimates of limit values for stator current harmonics $(I_{\mathrm{G}(n)\mathrm{eff}}^{(\mathrm{lim})})$, calculated as per expression (9); values of stator current harmonics $(I_{\mathrm{G}(n)\mathrm{eff}})$, determined by Fig. 5, b; and current harmonics $(I_{\mathrm{OHL}(n)\mathrm{eff}})$ in adjacent overhead lines, calculated as per expression (10).

Table 1. Numerical values of harmonics of the magnetizing current, stator current, and current of adjacent overhead lines.

No.	Harmonic number	0	1	2	3	4	5	6	7	8	9	10
1	$I_{\mu(n)\mathrm{eff}}$, A	80	108.68	95.64	78.21	58.69	40.21	23.91	15.22	9.78	8.7	4.35
2	$I_{\mathrm{G}(n)\mathrm{eff}}^{(\mathrm{lim})}$, A	0	3,943.7	3,470.6	0	2,129.65	1,459.2	0	552.17	354.9	0	157.8
3	$I_{\mathrm{G}(n)\mathrm{eff}}$, A	0	5,273	2,531	0	1,133.7	184.55	0	0	0	0	0
4	$I_{\mathrm{OHL}(n)ef}$, A	80	38	25.9	0	27.45	31.13	0	15.22	9.78	0	4.35

For higher harmonics $(n \geq 2)$the data presented in Table 1 allow us to note a distinctive feature, which is that the emission of magnetizing current into the circuit of adjacent overhead lines increases with the harmonic number. This is due to the fact that increasing the number of the harmonic increases the capacitive susceptance of adjacent overhead lines and inductive reactance of stator windings.

As expected, the dominant one is the fundamental frequency of the stator current (5272.9 A, 50 Hz), which underpins the energy process of active and reactive power output by the synchronous generator. At the same time, the active component of the stator current (4,607 A) remains unchanged, since the turbine power does not change during the entire interval affected by the test GIC event, while the reactive component of the stator current reaches the value of 2,565.09 A.

However, deviations from the pure sine wave of the stator current, quantified as the distortion factor THD=52.68% (Fig. 5, b), proves a serious hazard. When estimating the permissible deviations from the pure sine wave of the stator current, additional loss from higher harmonic components should not be higher than the loss from negative sequence currents [18]. In particular, in compliance with GOST 533-2000, the maximum permissible level of long-term negative sequence currents must be 5% of the rated stator current [19]. For the TVF-2-100 turbo generator, the maximum permissible long-term current of the negative

sequence is ≈344 A. The values of the 2nd (36.82% of rated stator current) and 4th (16.49% of rated stator current) stator current harmonics presented in Table 1 are many times higher than the permissible long-term value of the negative sequence current.

5 Conclusion

Synchronous generators with capacity over 30 MW provide for negative sequence current protection that initiates tripping either with an independent time delay in the case of indirect cooling of winding conductors or with a dependent characteristic of time delay in the case of direct cooling of winding conductors [20]. In this case, the negative sequence current protection that initiates tripping must be supplemented by a more sensitive signal-initiating device with a tripping current not exceeding the long-term permissible negative sequence current. Thus, the effect of a test GIC event, the intensity of which does not exceed the GICs observed in real life, induces large deviations from the pure sine wave of the stator current as soon 10 seconds into the test. This proves a serious hazard even for the underloaded turbo generator and can cause the negative sequence protection not only to issue a signal, but also to initiate the tripping.

References

1. Boteller D.H. Effects of geomagnetically induced currents in the BC Hydro 500 kV system. D.H. Boteller. IEEE Trans. Power Deliv. 1989. Vol.4, no. 1. pp. 818-823.
2. Kappenman J.G. Bracing for the Geomagnetic Storm. J.G. Kappenman, V.D. Albertson. IEEE Spectrum, 1990.Vol. 28, no. 3. pp. 27-33.
3. Walling R.A., Khan A.H. Characteristics of transformer exciting current during geomagnetic disturbances. IEEE Trans on Power Delivery. 1991. vol. 6, No. 4, p.1707–1714.
4. Nobuo T., Tetsuo O., Fumihiko M., Sadamu S., Yasuo F. An experimental analysis of DC excitation of transformers by geomagnetically induced currents. IEEE Transaction on Power Delivery, 1994, vol.9, No. 2. P.1173-1179.
5. Picher P., Bolduc L., Dutil A., Pham V.Q. Study of the acceptable DC current limit in core-form power transformers. IEEE Transactions on Power Delivery, Vol.12, No.1, January 1997, p.257-265.
6. Sivokon', V.P. Higher harmonics as an indicator of geomagnetically-induced currents. V.P. Sivokon', A.S. Serovetnikov, A.V. Pisarev. ELEKTRO. Elektrotekhnika, elektroenergetika, elektrotekhnicheskaya promyshlennost'. 2011. No. 3. Pp. 30-34. (in Russian)
7. Kuvshinov A.A., Vakhnina V.V., Chernenko A.N., Rybalko T.A. Analytical model for magnetizing current harmonic emission by a power transformer under quasi-constant currents. Russian Electrical Engineering. 2017. No. 5. Pp.25-31. (in Russian)
8. Power transformers. Reference handbook. Ed. by S.D. Lizunov, A.K. Lokhanin. Moscow: Energoizdat, 2004. - 616 p. (in Russian)
9. Leites L.V. Electromagnetic analysis of transformers and reactors. Moscow: Energiya, 1981.- 392 p. (in Russian)
10. Chernykh I.V. Modeling of electrical devices in MATLAB. SimPowerSystems and Simulink. Moscow: DML Press, 2012. – 288 p. (in Russian)
11. Albertson, V.D. Measurement and instrumentation for disturbance monitoring of geomagnetic storm effects. Effects of solar-geomagnetic disturbances on power systems,

IEEE Publication 90TH0291-5 PWR, Special Panel Session REPORT, IEEE PES Summer Meeting, 1989.

12. Selivanov, V.N. Results of long-term logging of currents at neutrals of power transformers. V.N. Selivanov, A.N. Danilin, V.V. Kolobov, Y.A. Sakharov, M.B. Barannik. Transactions of the Kola Science centre, RAS. 2010 (1). No. 1, Issue 1. Series 19: Energy Technology. Pp. 84-90. (in Russian)
13. Elovaara J., Lindblad P., Viljanen A., Makinen T., Pirjcba R., Larssen S., Rielen B, Geomagnetically induced currents in the Nordic power system and their effects on equipment, control, protection and operation. CIGRE paper N36-301, CIGRE General Sessun 1992, Paris, France, August 31 September 5, 1992, 10p.
14. Barannik M.B., Danilin A.N., Katkalov Yu.V., Kolobov B.B., Sakharov U.A., Selivanov V.N. System of logging of geomagnetically induced currents in the neutrals of power transformers. Instruments and Experimental Techniques. 2012. No. 1. Pp. 112-123. (in Russian)
15. IEEE Guide for Establishing Power Transformer Capability while under Geomagnetic Disturbances. IEEE Std.C57.163-2015.
16. Anisotropic cold rolled electrical steel plates. Product catalog. Novolipetsk Steel (NLMK), 2018.
17. Kuvshinov A.A., Vakhnina V.V., Chernenko A.N., Pudovinnikov R.N. Reactive load of a synchronous generator during saturation of the core of a unit transformer induced by quasi-permanent currents. Industrial Power Engineering. 2021. No.4. Pp.11-19. (in Russian)
18. Kogan F.L. Abnormal operating conditions of high-capacity turbo generators. Moscow: Energoatomizdat, 1988. 192 p. (in Russian)
19. GOST 533-2000 (IEC 34-3-88). Rotating electrical machinery. Turbo-generators. General specifications
20. Requirements for Electrical Installations. Ministry of Energy of the Russian Federation. Revised and expanded 7th edition. Moscow: ZAO Energoservis, 2002. 275 p. (in Russian)